Selection of Muscle-Activity-Based Cost Function in Human-in-the-Loop Optimization of Multi-Gait Ankle Exoskeleton Assistance

Hong Han, Wei Wang, Fengchao Zhang, Xin Li, Jianyu Chen, Jianda Han, and Juanjuan Zhang

***Abstract*— Using "human-in-the-loop" (HIL) optimization can obtain suitable exoskeleton assistance patterns to improve walking economy. However, there are differences in these patterns under different gait conditions, and currently most HIL optimizations use metabolic cost, which requires long periods to be estimated for each control law, as the physiological objective to minimize. We aimed to construct a muscle-activity-based cost function and to find the appropriate initial assistance patterns in HIL optimization of multi-gait ankle exoskeleton assistance. One healthy subject walked assisted by an ankle exoskeleton under nine gait conditions and each condition was the combination of different walking speeds, ground slopes and load weights. Ten assistance patterns were provided for the subject under each gait condition. Then we constructed a cost function based on surface electromyography signals of four lower leg muscles and select the muscle weight combination by using particle swarm optimization algorithm to compose the cost function with maximum differences between different assistance patterns. The mean weights of medial gastrocnemius, lateral gastrocnemius, soleus and tibialis anterior activity under all gait conditions are 0.153, 0.104, 0.953 and 0.145, respectively. Then we verified the effectiveness of this cost function by optimization and validation experiments conducted on four subjects. Our results are expected to guide the selection of muscle-activity-based cost functions and improve the time efficiency of HIL optimization.**

***Index Terms*— "Human-in-the-loop" optimization, multi-gait, ankle exoskeleton, muscle activity, cost function.**

I. Introduction

NOWADAYS, wearable robotic devices, such as exoskeletons, have been widely used in military, medical and other fields. They can be used in performance augmentation of able-bodied individuals [1]– [5], rehabilitation training and locomotion assistance [6]. However, there are a large number of tunable controller parameters that dictate their behavior and their interaction with users in the devices, and it is a challenge to identify the best parameters for each individual.

"Human-in-the-loop" (HIL) optimization has been employed as a method to tune assistive device parameters on a subject-specific basis [7]. It is the process of iteratively and automatically generating exoskeleton assistance patterns to minimize a physiological cost function while an individual is using the device. Researchers have been able to obtain suitable exoskeleton assistance patterns during normal walking and have a significant improvement on walking economy by HIL optimization [8]– [13]. Although the studies have differed in their optimization algorithms and assistive device hardware, most of them used metabolic cost as the physiological objective to minimize because the amount of human energy consumption can reflect whether exoskeleton assistances have a positive effect on human during walking. For example, Zhang *et al.* used an unilateral ankle exoskeleton to assist plantar flexion during walking in HIL optimization and reduce the metabolic cost of 11 subjects by 24.2 ± 7.4% [9]; Ding *et al.* designed a bilateral hip exoskeleton which reduced the metabolic cost of 8 subjects by 17.4 ± 3.2% [11].

Cost functions based on human metabolic cost require long evaluation periods and contain substantial noise. An advanced measurement system for metabolic cost is indirect calorimetry, a method which estimates energetic cost using measurements of oxygen consumption and carbon dioxide production. The system usually comprises a flowmeter embedded in a rubber mask that covers the nose and mouth, which will cause discomfort if wearing the mask for a long time. While these systems are widely used, they are ill-suited for continuous use or long-term data collections, and current HIL optimization protocols still require 2-4 minutes to estimate the metabolic cost for each control law [7], [14]. Meanwhile, previous studies showed that there were differences in optimal exoskeleton assistance patterns obtained by HIL optimization among different subjects and under different gait conditions (different walking speeds, ground slopes and load weights) [9], [11], [13], so it will take much time to get the multi-gait suitable assistance patterns by HIL optimization based on metabolic cost. Therefore, it's necessary to explore whether other physiological responses can be used as optimization objectives. One reasonable choice is muscle activity, which measured by surface electromyography (EMG) that reflects

Manuscript received December 8, 2020; revised April 16, 2021; accepted May 17, 2021. Date of publication May 20, 2021; date of current version May 28, 2021. This work was supported in part by the National Key Research and Development Program of China under Grant 2017YFB1303005, in part by the National Natural Science Foundation of China under Grant 61703214 and Grant 62073179, and in part by the National Natural Science Foundation of Tianjin under Grant 17JCYBJC40600. *(Corresponding author: Juanjuan Zhang.)*

This work involved human subjects or animals in its research. Approval of all ethical and experimental procedures and protocols was granted by the Ethical Committee of Nankai University.

The authors are with the Tianjin Key Laboratory of Intelligent Robotics, Institute of Robotics and Automatic Information System, Nankai University, Tianjin 300350, China (e-mail: juanjuanzhang@nankai.edu.cn).

Digital Object Identifier 10.1109/TNSRE.2021.3082198

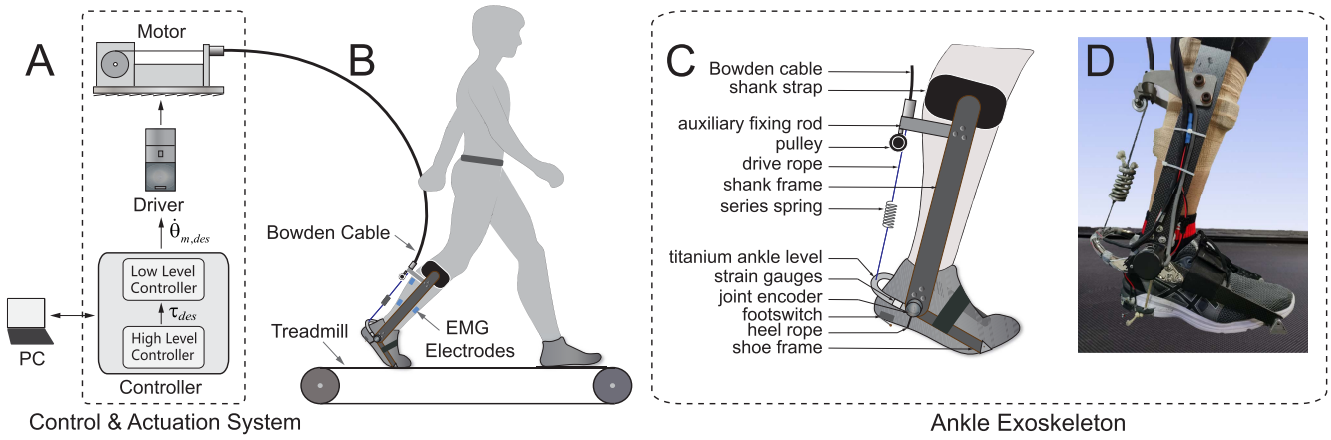

Fig. 1. Exoskeleton system. It includes a control system, a actuation system, transmissions and an ankle exoskeleton. (A) Control system and actuation system, consisting of a off-board real-time controller, a AC servo motor, a planetary gear and a motor driver. (B) Transmissions. A flexible unidirectional Bowden cable that is composed of a coiled-steel outer conduit and an inner rope is used as the transmission device between the motor and the exoskeleton worn on the leg. A series spring is attached at the end of the rope to improve the transmission compliance. (C) A enlarged schematic of the exoskeleton. (D) A photograph of the exoskeleton.

the energy consumption of muscle contraction. Steady EMG signals can be obtained with data collection for less time than using metabolic cost in each control law of HIL optimization. Nowadays, EMG signals have been widely used to control wearable robot devices [15]– [18], [27]], [28], [30].

Appropriate initial parameters of assistance patterns can substantially improve the time efficiency of multi-gait HIL optimization, and we can obtain them by firstly providing a variety of fixed assistance patterns with the individual and analyzing the changes of lower leg muscle activities under different assistance patterns for each gait condition. Meanwhile, we can construct a muscle-activity-based cost function with the experimental data.

Our goal was to construct a muscle-activity-based cost function in HIL optimization of multi-gait exoskeleton assistance and to provide a reference for the initial parameters selections of assistance patterns. We mainly focused on the lower leg muscles around ankle joint. This study was expected to help to evaluate exoskeleton performance and guide the selection of cost functions in HIL optimization. The results can be also used to improve the time efficiency of multi-gait HIL optimization by providing a good initial parameter estimate.

II. Methods

We firstly constructed a cost function on the basis of one subject's EMG signals of 4 lower leg muscles under different ankle exoskeleton assistance patterns under 9 gait conditions in TABLE I. We used statistical methods to identify the best weighted combination of muscle activities that differentiate different assistance the most. Then we recruited four subjects and used our cost function to carry out HIL optimization under different gait conditions to verify its effectiveness. Finally, we calculated cost function values under all gait conditions to provide a reference for the initial parameter identification of assistance patterns. All participants were provided with written informed consent before completing the protocol, which was approved by the ethical committee of Nankai University.

TABLE I
NINE GAIT CONDITIONS IN EXPERIMENTS

Gait Name	Speed (m/s)	Slope (%)	Load (kg)
Slow Walking (SW)	0.85	0	0
Normal Walking (NW)*	1.25	0	0
Fast Walking (FW)	1.65	0	0
6% Uphill Walking (UW6)	1.25	6**	0
12% Uphill Walking (UW12)	1.25	12	0
10 kg Loaded Walking (LW10)	1.25	0	10
20 kg Loaded Walking (LW20)	1.25	0	20
Slow 12% Uphill Walking (SUW12)	0.85	12	0
Fast 12% Uphill Walking (FUW12)	1.65	12	0

* Normal Walking is the control group of all gait conditions.
** Slope: 6% = 3.42°, 12% = 6.84°.

A. Exoskeleton System

We built an ankle exoskeleton system, including a off-board real-time control system and actuation system, a Bowden cable transmission with a series spring, and an ankle exoskeleton that interacted with the human foot and shank (Fig. 1).

We used a real-time control system (DS1202, dSPACE, Paderborn, GmbH) to sample sensors at 5000 Hz. The motor unit consisted of a AC servo motor, a 5:1 planetary gear and a motor driver (BSM90N-175AA, GBSM90-MRP120-5 and MF180-04AN-16A, ABB, Zurich, Swiss). The high-level controller was used to determine the desired torque. The low-level controller commanded desired motor velocity (Fig. 1A). A Bowden cable that was composed of a coiled-steel outer conduit and an inner rope was used as the transmission device between the motor and the exoskeleton. A series spring was attached at the end of the rope to improve the transmission compliance (Fig. 1B). The exoskeleton end-effector exerted forces on the front of the shank below the knee, beneath the heel, and on the ground beneath the toes, which produced the ankle plantar flexion torque. A Wheatstone bridge consisting of four strain gauges that were fixed on a

titanium level behind the heel measured the tension in the drive rope. The exoskeleton was integrated with a running shoe. A footswitch was installed on the sole to sense the instant of heel strike at the beginning of the gait cycle. There was a rope placed to the bottom of the shoe to lift the heel when providing assistive torque. Two digital optical encoders (E5, US Digital, WA, USA) were installed on motor shaft and exoskeleton joint shaft respectively to measure motor position and ankle joint angle (Fig. 1C, 1D).

B. Torque Control

We defined the desired exoskeleton plantar flexion assistive torque curve as an unimodal curve (Fig. 2B) by mimicking the human internal joint moment (Fig. 2A). This method of emulating human torques had been used and proved effective in multiple prior publications [9], [13]. The curve was constructed using four parameters: (1) peak time t_p, that was normalized to stride period and referred to the time when the exoskeleton provided the maximum assistive torque; (2) peak torque τ_p, which referred to the maximum assistive torque provided by the exoskeleton; (3) rise time t_r; (4) fall time t_f. One previous study showed that t_r and t_f had less obvious influence on the assistance effect of exoskeleton [9], so we took t_p and τ_p as the main assistance parameters and set t_r and t_f as the average optimization results of 11 subjects in [9]: 22.8% and 11.7%, respectively.

The desired assistive torque was tracked using a combination of proportional control, damping injection and iterative learning. The torque control method did not rely on explicit models or integration, which made it suitable for the complex, nonlinear and time-varying dynamics of human interaction with exoskeletons during walking [9]. The desired motor displacement $\Delta\theta_{m,des}(i,n)$ and commanded motor velocity $\dot{\theta}_{m,des}(i,n)$ were defined as follows [15], [16]:

$$\begin{aligned}
\Delta\theta_{m,des}(i,n) &= \Delta\theta^{LRN}_{m,des}(i+D,n) - K_p \cdot e_\tau(i,n) \\
&\quad - K_d \cdot \dot{\theta}_m(i.n) \\
\Delta\theta^{LRN}_{m,des}(i,n+1) &= \beta \cdot \theta^{LRN}_{m,des}(i,n) - K_l \cdot e_{flt}(i,n) \\
e_{flt}(i,n) &= (1-\mu)\cdot e_{flt}(i,n-1) + \mu \cdot e_\tau(i,n) \\
\dot{\theta}_{m,des}(i,n) &= \frac{1}{T} \cdot \Delta\theta_{m,des}(i,n) \qquad (1)
\end{aligned}$$

where i is the time index or number of control cycles elapsed within this stride. n is this stride and $n+1$ is the next stride. $D = 0.018\,s$ is the time delay between commanding and achieving a change in motor position. $K_p = 8$ is a proportional gain and $K_d = 0.05$ is a damping gain. $e_\tau = \tau - \tau_{des}$ is torque error, τ is measured exoskeleton torque and τ_{des} is desired exoskeleton torque. θ_m is measured velocity of the motor pulley. $T = 0.05\,s$ is a gain related to the rise time of motor. The controller used the torque error of each step to update the feed-forward trajectory of the desired motor displacement next step. $\beta \in [0,1]$ is a weight on the learned trajectory. $K_l = 0.05$ is the iterative learning gain. Noise in the error signal leads to improper updates on the learned trajectory, which can excite unstable ripple formation. It can be reduced by filtering the error signal. e_{flt} is the filtered torque error trajectory, and $\mu \in [0,1]$ is a weight of learned error. The value of β and μ was 1 in experiments.

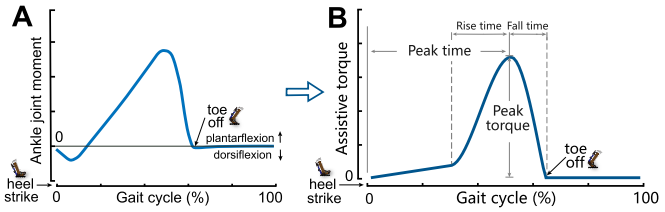

Fig. 2. (A) The human internal joint moment during a single gait cycle of ankle in sagittal plane. (B) Parameterization of ankle exoskeleton assistive torque. The assistive torque curve is defined by peak time, peak torque, rise time and fall time.

TABLE II
EXPERIMENT SEQUENCE

Exp Group Name	Gait Name	Note
Level Walking EXP	SW NW FW	**Speed: 0.85∼1.65 m/s** Slope = 0% Load = 0 kg
Uphill Walking EXP	NW UW6 UW12	Speed = 1.25 m/s **Slope: 0∼12%** Load = 0 kg
Loaded Walking EXP	NW LW10 LW20	Speed = 1.25 m/s Slope = 0% **Load: 0∼20 kg**
Incline Walking EXP	SUW12 UW12 FUW12	**Speed: 0.85∼1.65 m/s** Slope = 12% Load = 0 kg

C. Experimental Protocol

In cost function scanning experiments, we designed four groups of exoskeleton assistance walking experiments, including Level Walking EXP, Uphill Walking EXP, Loaded Walking EXP and Incline Walking EXP. (TABLE II). Each group of experiment was completed continuously and the interval of two groups was at least 48 hours to avoid the influence of fatigue. The walking speed and ground slope were changed by adjusting the speed and tilt angle of the treadmill, respectively. In Loaded Walking EXP, the subject wore a weighted running vest, and the load weight was evenly distributed in the front and back of the trunk.

One subject (male, 23 years, 180 cm, 58 kg) wore a right ankle exoskeleton and walked on a treadmill under ten different assistance patterns: zero torque (ZT), and combinations of three t_p and three τ_p levels (Fig. 3, p1 to p9) under each gait condition. According to previous studies, the ankle push-off time of most healthy subjects was between 45% and 53% of stride period [18], [20]. Therefore, we set the three t_p as 46%, 49% and 52% of stride period, respectively (early, middle and late t_p), which could distinguish different assistance patterns and were close to the optimal t_p in previous studies [9]. Considering that too high τ_p may lead to discomfort during walking, and assistance effects may not be obvious if τ_p was too small, we set the three τ_p levels as 20, 35 and 50 N·m (low,

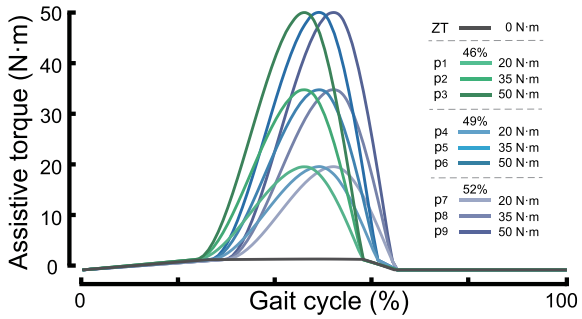

Fig. 3. Ten exoskeleton assistance patterns provided for the subject under each gait condition. ZT is zero torque. p1 to p9 is the nine exoskeleton assistance patterns (t_p / τ_p: 46 / 20, 46 / 35, 46 / 50, 49 / 20, 49 / 35, 49 / 50, 52 / 20, 52 / 35, 52 / 50, % Gait cycle / N·m).

medium and high τ_p) after doing the preliminary experimental test and training.

We used a wireless EMG system (Bagnoli, Delsys, MA, USA) to measure sEMG signals of four lower leg muscles (medial gastrocnemius: mGAS, lateral gastrocnemius: lGAS, soleus: SOL and tibialis anterior: TA) on the exoskeleton side. The four muscles we chose are mainly responsible for the plantarflexion and dorsiflexion movements of ankle joint. We placed EMG sensors in strict conformity with human anatomy, and we used stickers and bandages to make full contact between EMG sensors and the skin surface to avoid sensors falling off or losing contact with the skin during experiments. The wireless EMG system avoided the long-time wearing process and it only took about 5 minutes to wear EMG sensors. The original EMG signals passes through successively a 2nd-order Butterworth high-pass filter (cut-off frequency of 20 Hz), a full-wave rectification and a 2nd-order Butterworth low-pass filter (cut-off frequency of 10 Hz). In each group of experiment, all EMG amplitudes after preprocessing were normalized by the maximum under 30 assistance patterns (3 gait conditions $\times$ 10 assistance patterns). Our previous study showed that the root-mean-square (RMS) of EMG signals were well corrected with both mean and max values [21]. Meanwhile, it was recognized that a relatively linear relationship existed between RMS and muscle force [32], so RMS of EMG signals were selected as the primary index to estimate muscle activities. We used One-way Analysis of Variance (ANOVA) to analyze whether muscle activities under 9 assistance patterns reduced significantly compared to zero torque for each gait condition, and the significance level was set $\alpha = 0.05$.

Before experiments, 3 minutes was used to allow participants to getting used to wearing exoskeleton and make coarse estimation of t_p and τ_p ranges. In formal experiments, the subject firstly experienced zero torque pattern, and then was provided with 9 different assistance patterns in a random order. All patterns lasted for 2 minutes to ensure stable muscle activities and we recorded the measured data of the last 60 s in 2 minutes. The results are shown in Fig. 4.

D. Muscle-Activity-Based Cost Function

Using the EMG signals of four muscles under different assistance patterns, we constructed a muscle-activity-based cost function for multi-gait HIL optimization:

$$CF = g_1 \cdot mGAS + g_2 \cdot lGAS + g_3 \cdot SOL + g_4 \cdot TA \quad (2)$$

where, g_i $(i = 1, \ldots, 4)$ are the muscle activity weights that need to be optimized and $mGAS, lGAS, SOL, TA$ are RMS of EMG signals of four muscles in each gait cycle. EMG signals need be normalized by the maximum under zero torque condition.

When optimizing the muscle weights, we first set four muscles the same ranges of weights: g_1, g_2, g_3, $g_4 \in [0, 1]$. Considering the biomechanics and previous studies, GAS and SOL are mainly involved in human walking, running and jumping, so exoskeleton assistances maybe have a positive effect on the reduction of their activities, while TA is mainly used for dorsiflexion during walking, and uncomfortable exoskeleton plantarflexion assistance will increase its activity. Therefore, we set $g_4 \in [-1, 1]$ to maximize the difference between different assistance patterns.

There must be significant differences between the CF value in Eq(2) under different assistance patterns. Therefore, we desiged the optimization objective function from the perspective of statistics to get the optimal muscle activity weight combination. We expressed the cost function by matrix:

$$J_m = [g_1 \quad g_2 \quad g_3 \quad g_4] \cdot \begin{bmatrix} mGAS_1 & \cdots & mGAS_n \\ lGAS_1 & \cdots & lGAS_n \\ SOL_1 & \cdots & SOL_n \\ TA_1 & \cdots & TA_n \end{bmatrix} \quad (3)$$

where $mGAS_n$, $lGAS_n$, SOL_n and TA_n are RMS of EMG signals of four muscles in the n_{th} step. J_m is $1 \times n$ vector depositing cost function values under each assistance pattern. For each gait condition, $m = 1, \ldots, 9$ (except zero torque) and 36 P-values ($\sum_{i=1}^{8} i = 36$) were obtained by pairwise combination independent-samples t-test for J_1 to J_9. The average of logarithms of 36 P-values was used as the optimization objective J:

$$minimize \quad J = \frac{\sum_{j=1}^{36} lg(P_j)}{36} \quad (4)$$

For the nine gait conditions we set, we all used particle swarm optimization algorithm to minimize the objective J and obtained the optimal muscle activity weight combination. For NW and UW12, we took the average of multiple experiments as the final results under this gait condition. Finally, We used the average of weight combinations under nine gait conditions as the final weight combination in optimized cost function.

E. Verification

We recruited four subjects to participate in validation experiments under four different gait conditions. The validation experiments included two parts: HIL optimization and results validation.

Covariance Matrix Adaptive Evolution Strategy (CMAES) is stochastic, derivative-free, and it works for non-linear and non-convex continuous problems, which are beneficial to our issue, so we used it to minimize the cost function and obtained the optimized assistance pattern. In our previous study, SOL

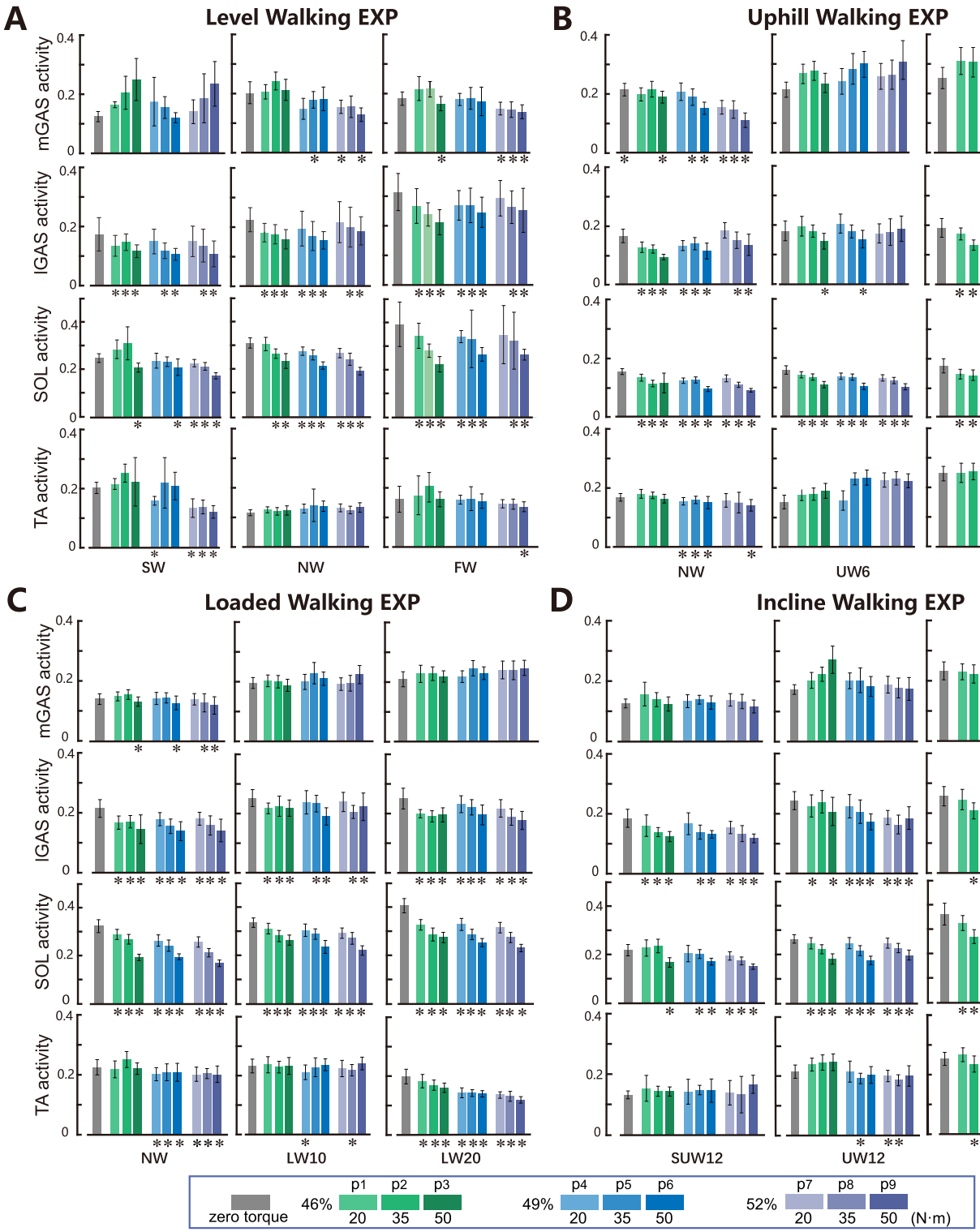

Fig. 4. Lower leg muscle activities over the whole stride under different exoskeleton assistance patterns for all gait conditions. (A) Level Walking EXP. (B) Uphill Walking EXP. (C) Loaded Walking EXP. (D) Incline Walking EXP. Muscle activities were normalized by the average of the 30 maximum values of muscle activities under 30 assistance patterns in each experiment. Bars and whiskers are means and standard deviations of muscle activities in all steps. $*$ represents that muscle activities reduced significantly compared to zero torque.

activity reduced more significantly compared to other muscles [21], and our ankle exoskeleton mainly replaced SOL contraction during walking. Therefore, we carried out validation experiments by comparing the results of HIL optimization based on the optimized cost function which was muscle activity weighted sums (CF-MAWS) with those based on only SOL activity (CF-SOL).

The optimization time was a key problem in HIL optimization, and previous studies had also confirmed that longer optimization time was not necessarily better, because subjects

TABLE III
THE MUSCLE ACTIVITY WEIGHT COMBINATION IN COST FUNCTION OBTAINED BY PSO

Gait Name	g_1	g_2	g_3	g_4	J
SW	0	0	0.707	1	−9.680
NW*	0.290	0.004	1	0.001	−12.005
FW	0.752	0.476	1	0.559	−4.018
UW6	0	0	0.730	−0.161	−13.441
UW12**	0.032	0.116	1	−0.032	−8.168
LW10	0	0.089	1	−0.102	−7.831
LW20	0	0.132	1	0.841	−10.157
SUW12	0.154	0.167	1	0.052	−8.229
FUW12	0	0.137	1	−0.222	−7.616
MEAN	**0.153**	**0.104**	**0.953**	**0.145**	**−9.363**

* The optimization results of 3 experiments in NW: Level Walking EXP: [0.281, 0.011, 1, −0.113, J = −11.043]; Uphill Walking EXP: [0.363, 0, 1, 0.024, J = −10.052]; Loaded Walking EXP: [0.226, 0, 1, 0.092, J = −14.918].

** The optimization results of 2 experiments in UW12: Uphill Walking EXP: [0.064, 0.119, 1, −0.116, J = −8.106]; Incline Walking EXP: [0, 0.114, 1, 0.052, J = −8.229].

were prone to fatigue, resulting in the changes in physical responses [9]. Therefore, we should choose the optimization time as short as possible. We tried to carry out CMAES optimization for 4 generations, which can achieve the desired effects. In each HIL optimization, we set the initial parameters which the subject felt comfortable with. We expected that the parameters were not far away from the optimum, so 4 generations of CMAES was sufficient for the optimization of 2 parameters (t_p, τ_p). The first generation was used to sample and evaluate the space from initial guess. The second generation was used to sample and evaluate the expanded space in case the optimum was not within the initial space. The third generation is expected to sample around the optimum with fairly large variance. The fourth generation was used to fine tune the estimation of the optimum [22]. An optimization experiment took 24 minutes, and more generations may cause muscle fatigue and affect the optimization results. Finally, each HIL optimization was carried out for 4 generations and two different optimized torques: OT-MAWS and OT-SOL can be obtained by HIL optimization based on CF-MAWS and CF-SOL, respectively.

In results validation, each subject experienced zero torque condition and two optimized assistive torques OT-MAWS and OT-SOL. To minimize the effects of adaptation and fatigue, the subject experienced the three assistance patterns again, but in the opposite order. All assistance patterns lasted for 2 minutes, and then the last 60 s of data were recorded. The validation experiment of each subject was completed within one day, during which the positions of EMG sensors were unchanged. We verified the effectiveness of our cost function by comparing the optimized CF value when the subject was provided with OT-MAWS and OT-SOL in results validation.

III. RESULTS

The results of optimized muscle activity weight combination are shown in TABLE III. The mean weights of mGAS, lGAS, SOL and TA activity under all gait conditions are 0.153, 0.104, 0.953 and 0.145, respectively and the mean optimized objective J is −9.363. The weight of SOL activity g_3 reaches its upper bound 1 under most gait conditions, while mGAS, lGAS and TA activities have the lower weight. CF-MAWS (optimized cost function) and CF-SOL can be expressed as:

$$\begin{aligned} CF-MAWS = {} & 0.153 \cdot mGAS + 0.104 \cdot lGAS \\ & +0.953 \cdot SOL + 0.145 \cdot TA \end{aligned} \tag{5}$$

$$CF-SOL = 0 \cdot mGAS + 0 \cdot lGAS + 1 \cdot SOL + 0 \cdot TA \tag{6}$$

where, $mGAS, lGAS, SOL, TA$ are RMS of EMG signals of four muscles in a gait cycle and EMG signals need be normalized by the maximum under zero torque condition for a certain gait condition. Using CF-MAWS and CF-SOL as the HIL optimization objective, the obtained exoskeleton assistance patterns of four subjects were: Subject1 under Normal Walking: OT-MAWS = [48.50%, 47.58 N·m], OT-SOL = [47.70%, 39.22 N·m]; Subject2 under Slow Walking: OT-MAWS = [50.00%, 34.16 N·m], OT-SOL = [50.37%, 32.39 N·m]; Subject3 under Uphill Walking (12%): OT-MAWS = [47.59%, 45.85 N·m], OT-SOL = [47.56%, 40.50 N·m]; Subject4 under Loaded Walking (5 kg): OT-MAWS = [50.27%, 33.89 N·m], OT-SOL = [48.87%, 35.20 N·m] (Fig. 5A). Optimized CF values of four subjects when they were provided with assistive torque OT-MAWS were lower than those when they were provided with OT-SOL. SOL activity were the same. Compared to zero torque condition, optimized CF values under four gait conditions reduced by 31.6%, 33.2%, 26.2% and 10.71%, respectively (Fig. 5B, 5C).

From optimized CF value under different gait conditions (Fig. 6), we obtained that the later t_p under slow walking or the earlier t_p under fast walking will produce the better effect of exoskeleton assistance. We also found t_p may be earlier with the increase of ground slopes and optimal assistance parameters were not sensitive to the change of load weights. For a certain gait, the drop amplitude of optimized CF value reached the maximum mostly when the subject was provided with the maximal τ_p (50 N·m) under three different t_p.

IV. DISCUSSION

Our first goal was to provide a method of constructing the muscle-activity-based cost function for multi-gait HIL optimization. We used scanning experiments data of one subject to get muscle activity weight combinations under each gait condition, and then used the average result of all gait conditions as the cost function for multi-gait HIL optimization. The reason why one subject participated was that the main purpose of this study was to reduce the experimental scales as much as possible, since the scanning of multi-gait, multi-assistance human responses took too long time (in total over 300 minutes of walking assisted by exoskeleton) and was not suitable for most participants, especially for gait-impaired patients. Therefore, we firstly tried to construct a cost function on the basis of single subject's data. Then we recruited other subjects and used our cost function to

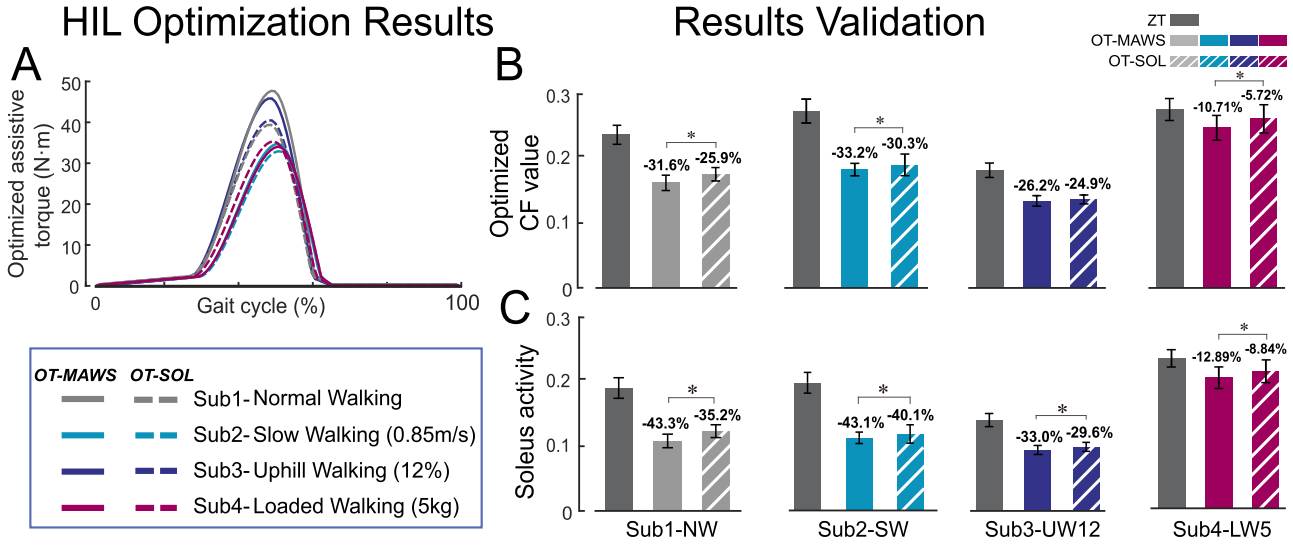

Fig. 5. Results of HIL optimization and results validation experiments of four subjects. (A) The optimized exoskeleton assistive torques in HIL optimization. OT-MAWS and OT-SOL are the optimized torques obtained by HIL optimization based on CF-MAWS and CF-SOL, respectively. (B) Optimized CF value when subjects were provided with zero torque (ZT), OT-MAWS and OT-SOL in results validation experiments. Bars and whiskers are means and standard deviations of optimized CF values in all steps. (C) Soleus activity when subjects were provided with zero torque, OT-MAWS and OT-SOL. Muscle activities are normalized by the maximum under zero torque condition under each gait condition. Bars and whiskers are means and standard deviations of muscle activities in all steps. $*$ represents statistically significant differences between optimized CF value or Soleus activity under OT-MAWS and that under OT-SOL (t-test, $\alpha = 0.05$).

carry out HIL optimization under different gait conditions to verify its effectiveness. In Fig. 5, optimized CF values of four subjects when they were provided with OT-MAWS were lower than those under OT-SOL, which showed that using our cost function produced assistance patterns that reduced more muscle activities and subjects felt more comfortable with. Meanwhile, it also added to the proof that our proposed cost function can be generalized to different subjects and gait conditions.

From the PSO results in TABLE III, we found that SOL activity weight reached its upper bound 1 under most gait conditions, which showed that the difference of its activity between different assistance patterns was the largest under these gait conditions. From the biomechanical point of view, SOL arises from the posterior surface of the tibia, fibula and the deep calf muscles and its tendons join with gastrocnemius to plantarflex the ankle [20]. The slow twitch fibers of SOL are more than fast twitch fibers and SOL is resistant to fatigue so as to involve in less intense sports such as standing, walking and jogging [20], [23]. Therefore, when the plantarflexion assistive torque was provided for ankle joint, it replaced the contraction of SOL, resulting in the reduction of muscle activities. This explanation also indicated that the exoskeleton assistance torque was consistent with the biomechanics of human walking.

mGAS and lGAS activities had the lower weights. Presumably it was because fast twitch fibers of GAS are more than those of SOL, and GAS are used for explosive activities with great strength, such as weight lifting, sprinting and jumping, but they seldom involves in walking. In particular, mGAS and lGAS activity showed the higher weights under FW ($g_1 = 0.752$, $g_2 = 0.479$), indicating that the contribution of GAS to human walking increased when fast walking, so the difference of their activities under different assistance patterns was more significant, which was consistent with our analysis.

The weight of TA activity g_4 was positive or negative, which showed that the subject maybe adopt different walking strategies to adapt to the change of assistance patterns under different gait conditions. g_4 did not reach the lower bound -1 (the minimum was -0.222), which indicated that the range of g_4 was feasible. When g_4 was negative, we found that the change trend of its activity under different assistance patterns was opposite to SOL activity. Therefore, TA can be regarded as a balance term in cost function. TA has antagonistic effect on exoskeleton assistance, and the application of inappropriate slightly assistive torque may increase its activity. However, the results in Fig. 4 showed that its activity reduced significantly compared to zero torque ($P < 0.05$) when the subject was provided with assistive torque with late t_p under SW and all assistance patterns under LW20. Accordingly, g_4 reached the maximum under the two gait conditions (SW: $g_4 = 0.841$, LW20: $g_4 = 1$). The possible reason was that when slow walking, the subject was more relaxed so that it was not necessary to quickly lift the foot to get a ground clearance, and the late t_p was more suitable for SW. Under LW20, muscle fatigue slowed the footstep, which will weaken the antagonism of TA to assistive torques from the exoskeleton.

Current HIL optimization protocols require around 2 minutes to estimate the metabolic cost for each control law [7], [9], [14], so it will take at least 48 minutes to complete CMAES optimization for 4 generation (6 control laws per generation), and it is only in the case of two-parameter optimization and single joint assistance. More parameters and numbers of joint assistance will led to longer periods for

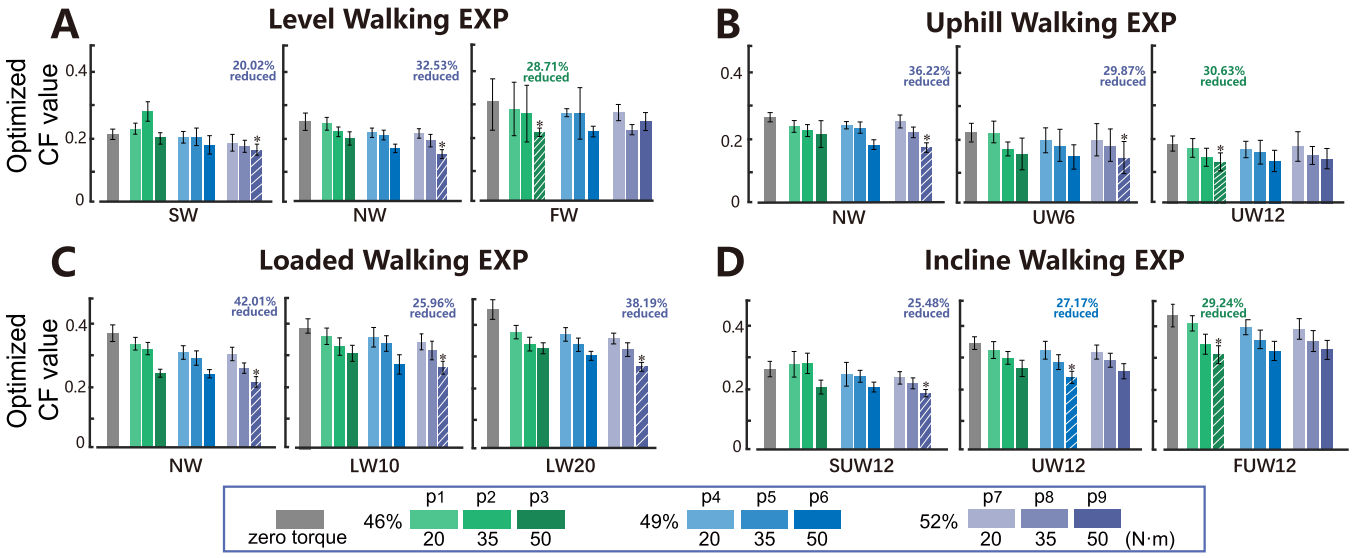

Fig. 6. Optimized cost function value over the whole stride under different exoskeleton assistance patterns for all gait conditions. (A) Level Walking EXP. (B) Uphill Walkling EXP. (C) Loaded Walking EXP. (D) Incline Walking EXP. Bars and whiskers are means and standard deviations of it in all steps. $*$ represents that it reduced significantly compared to zero torque. Shadow represents that it is the lowest under this assistance pattern. The numbers above the bars represent the reduction percentage of optimized CF value compared to zero torque.

HIL optimization, which is impractical for patients. EMG signals need less estimation time (about 40 s) than metabolic cost. We collected EMG signals for 60 s for each control law, so using our cost function can reduce the time needed by 50% compared to HIL optimization based on metabolic cost.

Our second goal was to find the appropriate initial assistance patterns in multi-gait HIL optimization, which will lead to less optimization generation of CMAES. We calculated optimized CF value with the mean weight combination [0.153, 0.104, 0.953, 0.145] to find the appropriate initial values of t_p and τ_p under different gait conditions (Fig. 6). In Level Walking EXP, optimized CF value was the lowest in p9 (late t_p, high τ_p) under SW, and it reduced by 20.02% compared to zero torque (the same below). While under FW, it was the lowest at p3 (early t_p, high τ_p), reducing by 28.71%. When walking at normal speed, it was the lowest in p9 too, reducing by 32.53%, but the difference between it in p9 and in p6 (middle t_p, high τ_p) was smaller, so the effect of assistance patterns with later t_p under slow walking or earlier t_p under fast walking will be better. In Uphill Walking EXP, with the increase of slope from 6% to 12%, optimized CF value changed from the lowest in p9 to in p3, reducing by 29.87% and 30.63%, respectively. Under UW6, there was little difference between the optimized CF value in p6 and that in p9 (p6: 0.1839 $\pm$ 0.0151; p9: 0.1738 $\pm$ 0.0123), so with the increase of ground slope, t_p maybe earlier, but it depended on the subject's walking strategy. When the strategy of increasing the stride frequency and decreasing the stride length was adopted to adapt to the uphill gait condition, it may be necessary to set t_p earlier. On the contrary, t_p should be later. In Loaded Walking EXP, the change of load weights did not change the distribution of optimized CF value under nine assistance patterns and it was all the lowest in p9, with the reduction of 42.01% (NW), 25.96% (LW10) and 38.19% (LW20), respectively. Therefore, assistive torque parameters were not sensitive to the change of load weights. In Incline Walking EXP, when the subject went up 12% slope at slow speed, normal speed and fast speed, the lowest optimized CF value occurred in p9, p6 and p3, reducing by 25.48%, 27.17%, and 29.24%, respectively. These results suggested that t_p may be the determinant of the effect of exoskeleton assistance under multi-gait conditions.

From HIL optimization results in Fig. 5, t_p of optimized assistive torque was earlier (about 47%) under UW12, while it was later (about 50%) under SW, which was consistent with above conclusions. Meanwhile, it did not need too high τ_p under SW. Under UW12 and LW5, the decrease of optimized CF value under OT-MAWS was smaller than that under NW. We did not choose high enough slopes and load weights, so optimized CF value may have a higher decrease under gait conditions with higher slopes and load weights.

V. Conclusion

We presented a method to construct a muscle-activity-based cost function and used it to provide a reference for the initial parameter identification of assistance patterns in HIL optimization of multi-gait ankle exoskeleton assistance. EMG signal over metabolic cost was selected to reflect the human performance to avoid long evaluation periods. We used statistical methods to identify the best weighted combination of lower leg muscle activities that differentiate different ankle exoskeleton assistance the most. It provided evidence and guidance to cost function selection in HIL optimization of ankle exoskeleton customization under different gait conditions. The results are expected to help improving the efficiency of HIL optimization for lower-limb exoskeletons.

For future works, we plan to establish a more accurate muscle-activity-based cost function by comparing the relationship between metabolic cost and lower leg muscle activities under multiple gait conditions, and we will recruit more

subjects to carry out HIL optimization to build a multi-gait optimal assistance parameter model of ankle exoskeletons.

REFERENCES

[1] J. Ghan and H. Kazerooni, "System identification for the Berkeley lower extremity exoskeleton (BLEEX)," in *Proc. IEEE Int. Conf. Robot. Autom. (ICRA)*, May 2006, pp. 2477–2484.

[2] G. Aguirre-Ollinger, J. E. Colgate, M. A. Peshkin, and A. Goswami, "Active-impedance control of a lower-limb assistive exoskeleton," in *Proc. IEEE 10th Int. Conf. Rehabil. Robot.*, Jun. 2007, pp. 188–195.

[3] A. B. Zoss, H. Kazerooni, and A. Chu, "Biomechanical design of the berkeley lower extremity exoskeleton (BLEEX)," *IEEE/ASME Trans. Mechatronics*, vol. 11, no. 2, pp. 128–138, Apr. 2006.

[4] K. Suzuki, G. Mito, H. Kawamoto, Y. Hasegawa, and Y. Sankai, "Intention-based walking support for paraplegia patients with robot suit HAL," *Adv. Robot.*, vol. 21, no. 12, pp. 1441–1469, Jan. 2007.

[5] W. Cloud, "Man amplifiers: Machines that let you carry a ton," *Popular Sci.*, vol. 187, no. 5, pp. 70–73, 1965.

[6] S. Jezernik, G. Colombo, T. Keller, H. Frueh, and M. Morari, "Robotic orthosis lokomat: A rehabilitation and research tool," *Neuromodulation, Technol. Neural Interface*, vol. 6, no. 2, pp. 108–115, Apr. 2003.

[7] K. A. Ingraham, D. P. Ferris, and C. D. Remy, "Evaluating physiological signal salience for estimating metabolic energy cost from wearable sensors," *J. Appl. Physiol.*, vol. 126, no. 3, pp. 717–729, Mar. 2019.

[8] J. R. Koller *et al.*, "'Body-in-the-loop' optimization of assistive robotic devices: A validation study," in *Proc. Robot., Sci. Syst.*, 2016, pp. 1–10.

[9] J. Zhang *et al.*, "Human-in-the-loop optimization of exoskeleton assistance," *Science*, vol. 356, pp. 1280–1284, Jun. 2017.

[10] M. Kim *et al.*, "Human-in-the-loop Bayesian optimization of wearable device parameters," *PLoS ONE*, vol. 12, no. 9, Sep. 2017, Art. no. e0184054.

[11] Y. Ding, M. Kim, S. Kuindersma, and C. J. Walsh, "Human-in-the-loop optimization of hip assistance with a soft exosuit during walking," *Sci. Robot.*, vol. 3, no. 15, Feb. 2018, Art. no. eaar5438.

[12] R. W. Jackson and S. H. Collins, "Heuristic-based ankle exoskeleton control for co-adaptive assistance of human locomotion," *IEEE Trans. Neural Syst. Rehabil. Eng.*, vol. 27, no. 10, pp. 2059–2069, Oct. 2019.

[13] K. A. Witte, P. Fiers, A. L. Sheets-Singer, and S. H. Collins, "Improving the energy economy of human running with powered and unpowered ankle exoskeleton assistance," *Sci. Robot.*, vol. 5, no. 40, Mar. 2020, Art. no. eaay9108.

[14] J. C. Selinger and J. M. Donelan, "Estimating instantaneous energetic cost during non-steady-state gait," *J. Appl. Physiol.*, vol. 117, no. 11, pp. 1406–1415, Dec. 2014.

[15] J. Zhang, C. C. Cheah, and S. H. Collins, "Experimental comparison of torque control methods on an ankle exoskeleton during human walking," in *Proc. Int. Conf. Robot. Automat.*, May 2015, pp. 5584–5589.

[16] J. Zhang, C. C. Cheah, and S. H. Collins, "Torque control in legged locomotion," in *Bioinspired Legged Locomotion*, 2017, ch. 5, pp. 375–428.

[17] K. A. Witte, J. Zhang, R. W. Jackson, and S. H. Collins, "Design of two lightweight, high-bandwidth torque-controlled ankle exoskeletons," in *Proc. IEEE Int. Conf. Robot. Autom. (ICRA)*, May 2015, pp. 1223–1228.

[18] R. W. Jackson and S. H. Collins, "An experimental comparison of the relative benefits of work and torque assistance in ankle exoskeletons," *J. Appl. Physiol.*, vol. 119, no. 5, pp. 541–557, Sep. 2015.

[19] Y. Han and X. Wang, "The biomechanical study of lower limb during human walking," *Sci. China Technol. Sci.*, vol. 54, no. 4, pp. 983–991, Apr. 2011.

[20] M. W. Whittle, Ed., *An Introduction to Gait Analysis*, 4th ed. Oxford, U.K.: Butterworth-Heinemann, 2004.

[21] W. Wang, J. Chen, Y. Ji, W. Jin, J. Liu, and J. Zhang, "Evaluation of lower leg muscle activities during human walking assisted by an ankle exoskeleton," *IEEE Trans. Ind. Informat.*, vol. 16, no. 11, pp. 7168–7176, Nov. 2020.

[22] J. Zhang, *Towards Systematic Controller Design in Rehabilitation Robots*. Pittsburgh, PA, USA: Carnegie Mellon Univ., 2016.

[23] F. C. Anderson and M. G. Pandy, "Individual muscle contributions to support in normal walking," *Gait Posture*, vol. 17, no. 2, pp. 159–169, Apr. 2003.

[24] S. H. Collins, M. B. Wiggin, and G. S. Sawicki, "Reducing the energy cost of human walking using an unpowered exoskeleton," *Nature*, vol. 522, no. 7555, pp. 212–215, Jun. 2015.

[25] G. Lee *et al.*, "Reducing the metabolic cost of running with a tethered soft exosuit," *Sci. Robot.*, vol. 2, no. 6, May 2017, Art. no. eaan6708.

[26] J. Kim *et al.*, "Reducing the metabolic rate of walking and running with a versatile, portable exosuit," *Science*, vol. 365, no. 6454, pp. 668–672, Aug. 2019.

[27] C. Fleischer and G. Hommel, "A human-exoskeleton interface utilizing electromyography," *IEEE Trans. Robot.*, vol. 24, no. 4, pp. 872–882, Aug. 2008.

[28] Y. Zhuang, S. Yao, C. Ma, and R. Song, "Admittance control based on EMG-driven musculoskeletal model improves the human–robot synchronization," *IEEE Trans. Ind. Informat.*, vol. 15, no. 2, pp. 1211–1218, Feb. 2019.

[29] J. C. Selinger, S. M. O'Connor, J. D. Wong, and J. M. Donelan, "Humans can continuously optimize energetic cost during walking," *Current Biol.*, vol. 25, no. 18, pp. 2452–2456, Sep. 2015.

[30] E. M. McCain *et al.*, "Mechanics and energetics of post-stroke walking aided by a powered ankle exoskeleton with speed-adaptive myoelectric control," *J. NeuroEng. Rehabil.*, vol. 16, no. 1, pp. 1–12, Dec. 2019.

[31] P. Malcolm, W. Derave, S. Galle, and D. De Clercq, "A simple exoskeleton that assists plantarflexion can reduce the metabolic cost of human walking," *PLoS ONE*, vol. 8, no. 2, Feb. 2013, Art. no. e56137.

[32] A. Christie, J. G. Inglis, G. Kamen, and D. A. Gabriel, "Relationships between surface EMG variables and motor unit firing rates," *Eur. J. Appl. Physiol.*, vol. 107, no. 2, pp. 177–185, Sep. 2009.

[33] S. Haddadin, A. Albu-Schaffer, A. De Luca, and G. Hirzinger, "Collision detection and reaction: A contribution to safe physical human-robot interaction," in *Proc. IEEE/RSJ Int. Conf. Intell. Robots Syst.*, Sep. 2008, pp. 3356–3363.